Title of paper

Fractone bulbs derive from ependymal cells and their laminin composition affects cell proliferation in the subventricular zone

Authors, institutional affiliations and complete mailing address

Marcos Assis Nascimento
Institute of Physiological Chemistry and Pathobiochemistry and Cells-in-Motion (CiM) Cluster of Excellence, University of Münster, 48149 Münster, Germany;
Institute of Biophysics, Federal University of Rio de Janeiro, 21941-902 Rio de Janeiro, Brazil.

Tatiana Coelho-Sampaio
Institute of Biomedical Sciences, Federal University of Rio de Janeiro, 21941-902 Rio de Janeiro, Brazil.

Lydia Sorokin
Institute of Physiological Chemistry and Pathobiochemistry and Cells-in-Motion (CiM) Cluster of Excellence, University of Münster, 48149 Münster, Germany.

Number of Figures:
7 Main Figures + 3 Supporting Figures

Corresponding author

Marcos Assis Nascimento (manascimento@biof.ufrj.br)
Address: Av. Carlos Chagas Filho 373, Centro de Ciências da Saúde, B-11, Rio de Janeiro, Brazil. Postal code: 21941-902

Key Words

Neural Stem Cells, Extracellular Matrix, Cell Division, Stem Cell Niche

Abstract

Fractones are extracellular matrix structures in the neural stem cell niche of the subventricular zone (**SVZ**). Their cellular origin and what determines their localization at this site is poorly studied and it remains unclear whether they influence neural stem and progenitor cells (**NSPCs**) formation, proliferation and/or maintenance. To address these questions, we analyzed whole mount preparations of the lateral ventricle by confocal microscopy using different extracellular matrix and cell markers, revealing laminin α5 as a major component of fractones, which were profusely distributed throughout the SVZ and appeared at the center of pinwheels, a critical site for adult neurogenesis. We demonstrate that fractones appear at the apical membrane of ependymal cells at the end of the first week after birth, and the use of transgenic mice lacking laminin α5 gene expression (*Lama5*) in endothelium and in FoxJ1-expressing ependymal cells, revealed ependymal cells as the source of laminin α5-containing fractones. Loss of laminin α5 from fractone bulbs correlated with an aberrant upregulation of laminin α2 and a two-fold increase in the proliferation of NSPCs, as determined by PH3 staining. These results indicate that fractones are a key component of the SVZ and that the laminin isoform composition at this site affects NSPC numbers.

Introduction

The subventricular zone (**SVZ**) is the largest and most studied neural stem cell niche in adult mice. Within this niche, neural stem and progenitor cells (**NSPCs**) contact the ependymal cell layer lining the ventricles (Doetsch et al., 1999) and the basement membranes (**BMs**) of blood vessels (Shen et al., 2008; Tavazoie et al., 2008). BMs are specialized extracellular matrix sheets, which in most tissues underlie endothelia and epithelial layers and ensheath nerves and muscle fibers, but in the SVZ appear in an unique punctate pattern. In the CNS, blood vessels are surrounded by two biochemically distinct BMs, one underlying the endothelium and one produced by astrocytes and deposited in the parenchymal BM (Sixt et al., 2001; Wu et al., 2009). Fractones are described to

emerge from capillaries as thin stems, which branch profusely and terminate as BMs bulbs at the ependymal layer (Leonhardt and Desaga, 1975; Mercier et al., 2002, 2011), thereby accounting for their punctate appearance. Laminins are the main functional constituents of BMs, acting as a molecular scaffold for its assembly and providing biological signals that control cell migration, differentiation and proliferation (Smyth et al., 1999). All members of the laminin family are heterotrimers composed of one α, one β and one γ chain that combine to form 16 distinct isoforms with tissue specific distributions and functions (Durbeej, 2010). The C-terminus of the 5 laminin α chains are key to laminin signaling, bearing in most isoforms the domains recognized by membrane receptors that regulate cellular adhesion, migration and division (Colognato and Yurchenco, 2000). Although it has been shown that fractone bulbs contain several laminin α chains, it is not yet clear if they are present in similar amounts (Kazanis et al., 2010). Laminins containing the α5 chain have been shown to be crucial for pluripotent stem cell survival and self-renewal *in vitro* (Hongisto et al., 2012; Miyazaki et al., 2012; Laperle et al., 2015) and for inhibiting the proliferation of keratinocytes *in vivo* (Wegner et al., 2016). The effects of fractones on NSPCs physiology has been attributed to the perlecan; however, this is based solely on its ability to bind growth factors, e.g. bFGF, BMP-4 and BMP-7, and to present them to contacting cells (Douet et al., 2012; Kerever et al., 2014; Mercier and Douet, 2014).

Despite growing evidence of the relevance of fractones in the SVZ (Kazanis et al., 2010; Mercier et al., 2012), a comprehensive understanding of their location is still lacking, in particular how fractones relate to NSPCs and pinwheels, critical structures for adult neurogenesis formed by NSPCs and ependymal cells at the ventricle wall (Mirzadeh et al., 2008). In addition, identifying the cells responsible for producing fractones and determining whether the laminin composition plays a role in SVZ physiology are crucial to understanding how stem cells are formed and maintained at this site.

Previous studies have identified interactions between $GFAP^{+}$ neural stem cells and pan-laminin+ fractones using electron microscopy and immunofluorescence stainings of coronal sections of the SVZ (Leonhardt and Desaga, 1975; Mercier et al., 2002, 2011). Although suitable for unveiling

the existence of such interactions, analyzes of thin tissue sections cannot fully address interactions between fractones and neural stem cells at the SVZ, due the filamentous nature of GFAP+ cells. We therefore here analyze the position of fractone bulbs using 3D reconstruction of immunofluorescently stained whole mounts of the lateral wall, revealing that fractones are most frequently located precisely at the center of pinwheels. To identify the cell responsible for producing fractone bulbs and to investigate whether its laminin composition is important for regulating NSPC proliferation in the SVZ, we analyzed mice lacking *Lama5* expression in endothelial cells, pericytes/smooth muscle or ciliated ependymal cells. Our data suggest that ependymal cells are the source of laminin α5-containing fractones, and demonstrated that the loss of laminin α5 at this site correlated with an aberrant upregulation of laminin α2 and a two-fold increase in the proliferation of NSPCs, as determined by PH3 staining. Our findings indicate that fractone bulbs are ependymally-derived basement membrane structures critical to SVZ physiology.

Materials & Methods

Experimental Animals. FoxJ1*/Lama5*$^{-/-}$ mice were obtained by crossing FoxJ1-Cre mice (Zhang et al., 2007) with *Lama5*$^{flox/flox}$ mice (Song et al., 2013); Tie2*/Lama5*$^{-/-}$ mice were obtained in analogous way (Song et al., 2013). *Lama4*$^{-/-}$ mice were previously described (Thyboll et al., 2002). All mice were on a C57BL/6 background (Charles River Laboratories). Male and female mice were used. Animal breeding and procedures were conducted according to the German Animal Welfare guidelines.

Histological Preparations. Brains were dissected and fixed overnight at 4°C in 2% paraformaldehyde in PBS. Thick (50 µm) coronal sections were made using a Zeiss Vibratome. Whole mounts were prepared from dissecting lateral walls of the lateral ventricles as described previously (Mirzadeh et al., 2008, 2010).

Antibodies & Imunohistochemistry. Sections and whole mounts were washed in PBS, blocked with 5% goat serum/PBS or 1% BSA/PBS (Sigma) and incubated with primary antibodies overnight at 4°C.

Primary antibodies used: Anti-laminin α2 (4H8-2) (Schuler and Sorokin, 1995) anti-laminin α5 (4G6) (Sorokin et al., 1997b), anti-laminin γ1 (3E10) (Sixt et al., 2001), anti-pan-laminin (455) (Sorokin, 1990), anti-β-catenin (Sigma cat.# C2206, 1:1000), anti-GFAP (Sigma cat.# C9205, 1:800; eBioscience cat.# 53-9892, 1:500), anti-nestin (rat-401, DSHB/Iowa 1:100), anti-PH3 (Millipore cat.# 06-570, 1:500). After the incubation, tissues were thoroughly washed with PBS and incubated with secondary antibodies: Alexa 488 anti-rat (Life Technologies cat.# A11006, 1:1000), Alexa 555 anti-rat (Abcam cat.# ab150154, 1:1000), Alexa 568 anti-rabbit (Life Technologies cat.# A11011 1:1000), Alexa 647 anti-rabbit (Jackson/Dianova cat.# 111-605-144 1:1000). After incubation with secondary antibodies, thick sections and whole mounts were mounted with mounting media and a coverslip. Tissues were analyzed using a Zeiss AxioImager microscope equipped with epifluorescent optics and documented with a Hamamatsu ORCA ER camera or with a Zeiss confocal laser scanning microscope LSM 700.

In situ hybridization. In situ hybridization for laminin α5 mRNA was performed as previously described (Sorokin et al., 1997a).

Morphological and Statistical Analyses. For PH3+ nuclei quantification, whole mounts were photographed with a 10x objective lens in the Zeiss AxioImager. Pictures were merged using Adobe Photoshop CS3 (Adobe Systems, Mountain View, CA). Merged pictures were processed using ImageJ (U.S. National Institutes of Health, Bethesda,MD, USA) and nuclei were quantified. Mice were age-matched (60 days old). For quantification of fractone bulbs volume, pan-laminin stainings in coronal sections were rendered in tridimensional volumes and quantified using Imaris 7.0 software (Bitplane). When comparing genotypes, mice were age-matched (~200 days old). For analyses of interactions of GFAP+ processes and bulbs in old mice, GFAP and pan-laminin stainings of whole mounts were reconstructed in 3D using Imaris. Statistical analyses were made using Graphpad Prism 6 (GraphPad Software Inc., La Jolla, CA). ANOVA with Bonferroni post test with a 95% confidence interval was used to analyze differences in number of nuclei positive for the PH3 proliferation marker.

Results

An en face view of interactions between GFAP+ cells and fractones.

In order to have a more comprehensive view of the interactions between neural stem cells (NSCs) and fractones, whole mounts of the SVZ were simultaneously immunofluorescently stained for laminin γ1 to mark BMs, GFAP to mark NSCs and β-catenin to reveal ependymal cells juctions. First, we observed that fractone bulbs comprise a significant part of all BM in the neurogenic niche (Fig. 1*A*), located between neighboring β-catenin+ ependymal cells (Fig. 1*B*). GFAP+ neural stem cells interact with BMs of blood vessels (Fig. 1*C*, *yellow arrowhead*) but their cell bodies and processes also contact several fractone bulbs at the same time (Fig. 1*C*, *arrowheads*).

NSCs exhibiting processes that contact the cerebrospinal fluid are the basic neurogenic unit in the SVZ and, together with surrounding ependymal cells, they form a distinct pinwheel-like arrangement (Mirzadeh et al., 2008). We observed that fractone bulbs are frequently at the center of pinwheels, where they contact neural stem cell bodies or processes (Fig. 1 *C-E,* Supp. 1). Fractone bulbs are located at the basolateral surface of ependymal cells, some are closer to the ventricular surface and can be found at the center of pinwheels (Fig. 1*F*, *surface*, *arrowheads*). These fractones seem to be preferentially contacted by GFAP+ processes (Fig. 1*F*, 6.2 *μm deep*, *arrowheads*). The labeled interactions (Fig. 1*F*, 1-3) between GFAP+ processes and fractone bulbs at pinwheels centers were reconstructed in 3D, indicating a direct contact between them.

Fractone bulbs are enriched in laminin α5.

Fractones are regarded as BM structures that emerge from capillaries as thin threads, known as stems, that branch out and reach the ependymal layer, where they become visible as spherical deposits known as bulbs (Mercier et al., 2002, 2011). We used monoclonal antibodies specific for each laminin α chain to investigate the isoforms present in fractone bulbs. We found that fractone bulbs exhibited strong laminin α5 staining, and only a few showed a weak immunoreactivity for the α2 chain (Fig.2, arrowheads). Laminin α4 was not found in any fractone bulb, in contrast to

129 previous reports (Kazanis et al., 2010). Laminin α1 and α3 chains were also completely absent in
130 bulbs (not shown), which is consistent with the literature (Kazanis et al., 2010).

131

132 **Fractone bulbs are produced by ependymal cells during the first week after birth.**

133 To determine when fractone bulbs form and whether this correlates with appearance of
134 laminin α5 expression, we investigated the emergence of fractones at the ependymal walls during
135 development. To do so, we checked the laminin isoform expression at the SVZ every day during the
136 first week after birth. Fractone bulbs, as defined by a punctate laminin γ1 staining, were not detected
137 at P0, however, in addition to blood vessel staining, a faint and disperse laminin γ1 chain staining
138 lining the ventricle was detectable at the nestin+ layer of late radial glial cells/early NSCs (Fig. 3*A*).
139 Laminin α5 expression in blood vessels in the CNS starts approximately at the third week after birth
140 (Sorokin et al., 1997b). However, in situ hybridization showed that mRNA for the laminin α5 chain is
141 already expressed at the ventricle surface (Fig. 3*B,* arrow) and choroid plexus at P0 (Fig. 3*B,*
142 arrowhead) as reported previously (Sorokin et al., 1997b). At P3, more condensed spots positive for
143 laminin γ1 and α5 were present in some regions of the ventricle (Fig. 3*C*). Laminin expression was
144 spatially heterogeneous, with dense laminin expression at regions of the dorsal wall while most
145 portions of the lateral wall lacked laminin immunoreactivity (Supp. 2). At P7, early laminin α5 and γ1
146 chain positive fractones were visible along all the ependymal surface of the lateral ventricles (Fig.
147 3*D*). In a frontal view of a P7 ependyma using a whole mount preparation, we observed that these
148 first fractones are small patches of BM at the apical surface of the ependymal cells, (Fig. 3*E*, *F*).
149 Analysis of FoxJ1-RFP reporter animals that express RFP under the control of the ependymal-specific
150 promoter FoxJ1, revealed laminin γ1 inside ependymal cells and some early fractones already at the
151 cell surface (Fig. 3*G*).

152 Fractones bulbs first appeared as small BM patches at the surface of ependymal cells,
153 indicating that these structures undergo major spatial and morphological changes until adulthood.

We therefore investigated whether fractone size changed over time by measuring their volumes in 3D stacks from confocal microscopy at P34, P86, P162, P175, P269 and P303. We observed that the mean volume increases gradually, showing a linear correlation with age (R^2=0.91). This result extends the recent observation that bulbs are larger in 100 week old mice than in 12 week-old mice (Kerever et al., 2015). A frequency distribution analysis showed that this increase in size occurs in the entire fractone population (Fig. 4*A, B*). Mice older than 200 days displayed large fractones (> 40 µm³) and were associated with more GFAP+ processes contacts than fractones in younger animals. In old mice (>200 days), the vast majority of fractone bulbs at pinwheel centers have a tunnel-like structure, allowing NSCs to extend their processes within these tunnels of basement membrane and reach the CSF (Fig. 4*C*). In addition, old mice had unique enlarged fractone bulbs, with some reaching over 20 µm in diameter (Fig. 4*D, arrowheads*). These giant fractones were associated with clusters of cells at the anterior ventral part of the ventricular wall (Fig. 4*D, arrows*). Such cell clusters were associated with both GFAP+ and GFAP- cells, and were surrounded by a strong β-catenin expression (Fig. 4*E, middle panels, red*). We also observed fragmented laminin deposits in their interior (Fig. 4*E, arrowheads*). Serial imaging through the giant pinwheels and 3D reconstruction revealed that the giant bulbs associated with these clusters were filled with GFAP+ processes that transverse them and reach more distant and smaller fractones (Fig. 4*F, top and bottom panels*). These data indicate that fractones are not static structures, since their size, shape, position and cellular interactions change gradually with age, becoming larger and more complex in old mice.

The early appearance of laminin α5 in fractones, before its expression is known to occur in association with CNS blood vessels (Sorokin et al., 1997b) suggests an ependymal source of laminin α5+ fractones. To more precisely investigate this possibility, we investigated laminin α5+ fractone bulbs in transgenic mice lacking the expression of *Lama5* in endothelium (Tie2/*Lama5*$^{-/-}$) and in ciliated epithelial cells include ependymal cells (Foxj1/*Lama5*$^{-/-}$). Tie2/*Lama5*$^{-/-}$ mice showed no changes in laminin α5 staining of fractone bulbs (Fig. 5*A*). We quantified the volumes of fractone

bulbs in 3D reconstructions of confocal stacks and we did not find any significant differences among these genotypes (31.11µm^3 ± 7.21 in WT vs. 29.22µm^3 ± 16.1 in Tie2/*Lama5*$^{-/-}$) (Fig. 5*B*), suggesting that endothelial cells are not the cellular source of fractone bulbs. However, Foxj1/*Lama5*$^{-/-}$ showed almost complete loss of laminin α5 staining at fractone bulbs by 1 month of age, and only very few small laminin α5+ fractones (Fig. 5*C*, *left panel, arrowheads*). The activation of FoxJ1 promoter starts at P0 and is one of the last maturation steps for ependymal cells, being temporally and spatially heterogeneous. The complete maturation for all ependymal cells do not occur before the third week after birth (Jacquet et al., 2009). Therefore, we investigated whether the few laminin α5-containing bulbs seen in Fig. 5*C* could have been produced before the deletion triggered by the FoxJ1 activation. To answer this, we analyzed the emergence of fractones and the expression of RFP in FoxJ1-RFP reporter mice. We found that in one-week old animals, some regions of the ventricle wall have a large number of RFP– cells (Fig. 5*D*, arrowheads). We also observed ependymal cells at different stages of late maturation: RFP+ cells with cilia, stained for acetylated tubulin (Fig. 5*E*, *arrows*), RFP+ cells without cilia (Fig. 5*E*, *filled arrowheads*) and RFP– cells (Fig. 5*E*, *hollow arrowheads*) at the ependymal wall that could be ependymal cells in a more immature phenotype. Although the vast majority of fractones were associated with RFP+ cells (Fig. 5*E*, and *arrows* in *F*), a few RFP– cells produced early fractones at their apical membrane (Fig. 5*F*, *arrowheads*), suggesting that while fractones production occurs at the late differentiation program of ependymal cells, there is temporal variation and a few ependymal cells can start producing fractones before FoxJ1 activation. To confirm this possibility, we investigated if laminin α5 containing bulbs were still present in Foxj1/*Lama5*$^{-/-}$ mice at two months of age, revealing no laminin α5 in fractones and expression only at in endothelial BMs (Fig. 5*G, center*).

Despite the lack of laminin α5 in Foxj1/*Lama5*$^{-/-}$ mice, fractone bulbs were still present as indicated by positive staining for other laminin chains, such as laminin γ1 (Fig 5*C*) and β1 chains and the other BM components such as collagen type IV and perlecan (not shown). Since laminins are heterotrimers, this finding suggests that other α chains could be expressed in fractones to

206 compensate for the lack of laminin α5. Screening for the expression of the other laminin α chains,
207 revealed upregulation of laminin α2 at fractones bulbs of Foxj1/*Lama5*$^{-/-}$ mice, which is almost absent
208 at this site in wild-type animals (Fig 5*F*).

209

210 **Foxj1/*Lama5*$^{-/-}$ mice exhibit increased cell proliferation in the SVZ.**

211 As laminin α5 has been shown to maintain embryonic stem cells in a non-differentiated state
212 and to regulate cell proliferation (Domogatskaya et al., 2008; Wegner et al., 2016), we investigated
213 whether the observed changes in laminin isoforms expression in the Foxj1/*Lama5*$^{-/-}$ could affect cell
214 proliferation in the SVZ. We compared the number of dividing cells in the SVZ, as assessed by
215 phospho-histone H3 (PH3) staining in whole mounts lateral wall preparations in WT mice and the
216 Foxj1/*Lama5*$^{-/-}$ mice, revealing a significant increase in numbers of dividing cells when laminin α5 was
217 absent from the fractone bulbs (157.5 +- 25.1 vs. 303.8 +- 20.9, p=0.0027) (Fig. 6 *A, B*). However,
218 *Lama4*$^{-/-}$, which have a compensatory upregulation of laminin α5 in the endothelial BM, and
219 Tie2/*Lama5*$^{-/-}$, which lack this isoform in the endothelial BM, show proliferation levels in the SVZ
220 similar to the wild type (Supp. 3).

221

222 ## Discussion

223 We show here that a major component of the BM structure that comprises the fractone
224 bulbs at the SVZ is laminin α5 which is produced by the ependymal cells, and that the laminin isoform
225 content of fractones affects cell division in the SVZ. Deletion of the *Lama5* gene in ependymal cells
226 eliminated laminin α5 from fractone bulbs, leading to a compensatory expression of laminin α2 and
227 an associated increase in proliferating cells in the SVZ, as assessed by PH3+ nuclei quantification,
228 suggesting a role for laminins in NSPCs proliferation at this site.

Fractones have been described as structures that emerge from the BMs of blood vessels in the vicinity of the SVZ. Given their expression of laminin α5, which is expressed in the CNS mainly by endothelial cells and deposited into the endothelial BM (Sorokin et al., 1997, Sixt et al., 2001), it was logical to postulate endothelial cells as the source of fractones (Shen et al., 2008). However, in addition to endothelium, laminin α5 is one of the major BM components of epithelial cells (Sorokin et al., 1997a; b) and has been previously described to be expressed by choroid plexus epithelium (Sorokin et al., 1997b). The use of transgenic mice lacking laminin α5 from endothelial and ependymal cells revealed that the main source of laminin α5 and presumably also fractones are the ependymal cells lining the ventricle. We show here that fractones are often in the center of pinwheels, formed by adjacent ependymal cells, at the interface between neural stem cells and CSF, and that with age they increase in size and in the number of associations with the GFAP+ neural stem cells.

Our data also showed that changes in laminin isoforms in fractones affect cell proliferation in the SVZ. Loss of laminin α5 correlated with a broader expression of laminin α2 in fractones which was associated with increased numbers of proliferating cells in the SVZ. Since laminin α2 containing BMs also have perlecan as do all BMS, there is no reason to consider that the perlecan content of fractones in Foxj1/*Lama5*$^{-/-}$ would be affected. Hence, the capacity to accumulate and present proliferation-inhibiting molecules is probably not impaired and a direct signaling via laminin α5 is likely to lead an anti-proliferative signal. While the current data does not permit distinction between and anti-proliferative effect of laminin α5 or pro-proliferative effect of laminin α2, the former is consistent with data from other tissues suggesting that laminin α5 is a central factor in other stem cell niches. Stem cell niches in epithelia, bone marrow and the vascular niche in the hippocampus, are all rich in laminin α5 (Miner et al., 1997; Palmer et al., 2000; Kiel et al., 2005). Laminin α5 containing isoforms also inhibit differentiation of embryonic stem cells, maintaining them in an anti-proliferative early progenitory state, through integrin signaling (Domogatskaya et al., 2008; Rodin et al., 2010; Hongisto et al., 2012). Consistent with an anti-proliferative effect of laminin α5 on neural stem cells, integrin α6β1, which has a higher affinity for laminin α5 compared to laminin α2

containing isoforms (Nishiuchi et al., 2006), and alpha-dystroglycan, are also associated with fractones (Shen et al., 2008; Adorjan and Kalman, 2009) and are downregulated on neural stem cells upon activation (Codega et al., 2014). Delivery of antibodies against this integrin into the CSF leads to a loss of stem cell anchorage and increases proliferation in 50% of the neural stem cells (Shen et al., 2008). However, it was assumed that the endothelial BM was the main source of ligands for the integrin α6β1, even though it was not clear whether stem cell processes directly contact laminin α5 in the endothelial BM.

As part of the blood-brain barrier, astrocytes ensheath capillaries in the CNS and produce a parenchymal BM rich in laminin α2, concealing the endothelial BM from other cells in the brain parenchyma (Hallmann et al., 2005). It is not clear if neural stem cells, due their astrocytic phenotype, contribute to this parenchymal BM in the SVZ. In either scenario, the endothelial BM would not be fully available to integrin binding by neural stem cells. Consistent with this hypothesis, we found that the laminin composition in endothelial BMs does not affect proliferation in the SVZ, suggesting that fractones are the source of laminin α5 for NSPCs integrin signaling, not blood vessels. In addition, we show here that stem cells can establish far more contacts with fractones than with blood vessels. Hence, most of the exposed ligand for integrin α6β1 is the laminin α5 in fractone bulbs. We therefore propose that the integrin α6β1 positive neural stem cells interact with laminin α5 in the fractones, which maintains neural stem cell character and limits proliferation and differentiation.

We also showed that pinwheels, formed by adjacent ependymal cells, can accommodate fractones at their centers where neural stem cell processes contact the CSF. We presume that these fractones provide an adherence spot for ependymal cell bodies and the apical processes of neural stem cells. In addition, the pinwheel center is a privileged site for tuning stem cell behavior, since the primary cilia at the tip of the apical process works as a signaling hub (Ihrie and Alvarez-Buylla, 2011). Having a BM at this critical site may help to stabilize the apical process in contact with the ventricle, exposing it to growth factors accumulated in fractones and enabling molecules at very low concentrations in the CSF to regulate neurogenesis. This interaction between apical processes and

283 fractones increases in complexity during aging, as tunneled bulbs fully wrap the apical ending of stem
284 cells. We also observed an increase in size of fractone bulbs with increased age of mice, confirming
285 and extending recent findings which described a reduction in fractone bulb numbers with age
286 (Kerever et al., 2015). The observed correlation between enlarged bulbs and GFAP+ cells clusters,
287 which indicates that GFAP+ cells could participate in the merging of these structures, may result in
288 the reduced fractone number reported by Kerever and co-workers. Taken together with our findings,
289 which suggest an inhibitory effect of laminin α5 on proliferation, the fusion of fractone bulbs could
290 account for the age-related decline of neurogenesis.

291 In summary, our work shows that laminin α5-containing fractones are a critical element in the SVZ
292 niche, being part of pinwheels and modulating the proliferation of NSPCs. Our data suggest that
293 laminin α5 in fractones acts as a key stem cell niche factor. Further analyses of FoxJ1/*Lama5*$^{-/-}$ mice,
294 investigating the activation states of neural stem cells and changes in NSPC populations will aid in
295 understanding the exact role of laminin α5 in fractones.

296

297 Acknowledgements

298 Cells-in-Motion Cluster of Excellence (EXE1003) from the German Research Foundation. Brasilien-
299 Zentrum of WWU/ DAAD, Conselho Nacional de Desenvolvimento Científico e Tecnológico - Science
300 Without Borders Program (238147/2012-6) for the financial support. Dr. Eva Korpos for discussion,
301 Dr Bhavin Shah for help with whole mounts, Stefan Luetke Enking for technical assistance and Sandra
302 Black Culliton for the art in the last figure. *FoxJ1*^{Cre} mice were a generous gift from Dr. Martin Bähler.

303

304 References

305 Adorjan I, Kalman M. 2009. Distribution of beta-dystroglycan immunopositive globules in the
306 subventricular zone of rat brain. Glia 57:657–66.

307 Codega P, Silva-Vargas V, Paul A, Maldonado-Soto ARRR, DeLeo AMMM, Pastrana E, Doetsch F. 2014.
308 Prospective Identification and Purification of Quiescent Adult Neural Stem Cells from Their In
309 Vivo Niche. Neuron 82:545–559.

310 Colognato H, Yurchenco PD. 2000. Form and function: The laminin family of heterotrimers. Dev Dyn
311 218:213–234.

312 Doetsch F, Caillé I, Lim D a., García-Verdugo JM, Alvarez-Buylla a., Caille I, Lim D a., Garcia-Verdugo
313 JM, Alvarez-Buylla a. 1999. Subventricular zone astrocytes are neural stem cells in the adult
314 mammalian brain. Cell 97:703–716.

315 Domogatskaya A, Rodin S, Boutaud A, Tryggvason K. 2008. Laminin-511 but not -332, -111, or -411
316 enables mouse embryonic stem cell self-renewal in vitro. Stem Cells 26:2800–9.

317 Douet V, Arikawa-Hirasawa E, Mercier F, Eri A-H, Mercier F, Arikawa-Hirasawa E, Mercier F. 2012.
318 Fractone-heparan sulfates mediate BMP-7 inhibition of cell proliferation in the adult
319 subventricular zone. Neurosci Lett 528:120125.

320 Durbeej M. 2010. Laminins. Cell Tissue Res 339:259–268.

321 Hallmann R, Horn N, Selg M, Wendler O, Pausch F, Sorokin LM. 2005. Expression and function of
322 laminins in the embryonic and mature vasculature. Physiol Rev 85:979–1000.

323 Hongisto H, Vuoristo S, Mikhailova A, Suuronen R, Virtanen I, Otonkoski T, Skottman H. 2012.
324 Laminin-511 expression is associated with the functionality of feeder cells in human embryonic
325 stem cell culture. Stem Cell Res 8:97–108.

326 Ihrie R a, Alvarez-Buylla A. 2011. Lake-front property: a unique germinal niche by the lateral
327 ventricles of the adult brain. Neuron 70:674–86.

328 Jacquet B V, Salinas-Mondragon R, Liang H, Therit B, Buie JD, Dykstra M, Campbell K, Ostrowski LE,
329 Brody SL, Ghashghaei HT. 2009. FoxJ1-dependent gene expression is required for differentiation
330 of radial glia into ependymal cells and a subset of astrocytes in the postnatal brain.

Development 136:4021–4031.

Kazanis I, Lathia JD, Vadakkan TJ, Raborn E, Wan R, Mughal MR, Eckley DM, Sasaki T, Patton B, Mattson MP, Hirschi KK, Dickinson ME, ffrench-Constant C. 2010. Quiescence and activation of stem and precursor cell populations in the subependymal zone of the mammalian brain are associated with distinct cellular and extracellular matrix signals. J Neurosci 30:9771–81.

Kerever A, Mercier F, Nonaka R, Vega S, Oda Y, Zalc B, Okada Y, Hattori N, Yamada Y, Eri A-H, de Vega S, Oda Y, Zalc B, Okada Y, Hattori N, Yamada Y, Arikawa-Hirasawa E, Vega S, Oda Y, Zalc B, Okada Y, Hattori N, Yamada Y, Eri A-H, de Vega S, Oda Y, Zalc B, Okada Y, Hattori N, Yamada Y, Arikawa-Hirasawa E. 2014. Perlecan is required for FGF-2 signaling in the neural stem cell niche. Stem Cell Res 12:492–505.

Kerever A, Yamada T, Suzuki Y, Mercier F, Arikawa-Hirasawa E. 2015. Fractone aging in the subventricular zone of the lateral ventricle. J Chem Neuroanat 66-67:52–60.

Kiel MJ, Yilmaz ÖH, Iwashita T, Yilmaz OH, Terhorst C, Morrison SJ. 2005. SLAM family receptors distinguish hematopoietic stem and progenitor cells and reveal endothelial niches for stem cells. Cell 121:1109–1121.

Laperle A, Hsiao C, Lampe M, Mortier J, Saha K, Palecek SP, Masters KS. 2015. α-5 Laminin Synthesized by Human Pluripotent Stem Cells Promotes Self-Renewal. Stem Cell Reports 5:195–206.

Leonhardt H, Desaga U. 1975. Recent observations on ependyma and subependymal basement membranes. Acta Neurochir (Wien) 31:153–9.

Mercier F, Douet V. 2014. Bone morphogenetic protein-4 inhibits adult neurogenesis and is regulated by fractone-associated heparan sulfates in the subventricular zone. J Chem Neuroanat 57-58:54–61.

Mercier F, Kitasako JT, Hatton GI. 2002. Anatomy of the brain neurogenic zones revisited: Fractones and the fibroblast/macrophage network. J Comp Neurol 451:170–88.

356 Mercier F, Kwon YC, Douet V. 2012. Hippocampus/amygdala alterations, loss of heparan sulfates,
357 fractones and ventricle wall reduction in adult BTBR T+ tf/J mice, animal model for autism.
358 Neurosci Lett 506:208–13.

359 Mercier F, Schnack J, Saint M, Chaumet G. 2011. Neurogenesis in the Adult Brain I. (Seki T, Sawamoto
360 K, Parent JM, Alvarez-Buylla A, editors.). Tokyo: Springer Japan.

361 Miner JH, Patton BL, Lentz SI, Gilbert DJ, Snider WD, Jenkins NA, Copeland NG, Sanes JR. 1997. The
362 laminin α chains: Expression, developmental transitions, and chromosomal locations of α1-5,
363 identification of heterotrimeric laminins 8- 11, and cloning of a novel α3 isoform. J Cell Biol
364 137:685–701.

365 Mirzadeh Z, Doetsch F, Sawamoto K, Wichterle H, Alvarez-Buylla A. 2010. The subventricular zone en-
366 face: wholemount staining and ependymal flow. J Vis Exp:1–8.

367 Mirzadeh Z, Merkle FT, Soriano-Navarro M, Garcia-Verdugo JM, Alvarez-Buylla A. 2008. Neural stem
368 cells confer unique pinwheel architecture to the ventricular surface in neurogenic regions of the
369 adult brain. Cell Stem Cell 3:265–78.

370 Miyazaki T, Futaki S, Suemori H, Taniguchi Y, Yamada M, Kawasaki M, Hayashi M, Kumagai H,
371 Nakatsuji N, Sekiguchi K, Kawase E. 2012. Laminin E8 fragments support efficient adhesion and
372 expansion of dissociated human pluripotent stem cells. Nat Commun 3:1236.

373 Nishiuchi R, Takagi J, Hayashi M, Ido H, Yagi Y, Sanzen N, Tsuji T, Yamada M, Sekiguchi K. 2006.
374 Ligand-binding specificities of laminin-binding integrins: a comprehensive survey of laminin-
375 integrin interactions using recombinant alpha3beta1, alpha6beta1, alpha7beta1 and
376 alpha6beta4 integrins. Matrix Biol 25:189–97.

377 Palmer TD, Willhoite AR, Gage FH. 2000. Vascular niche for adult hippocampal neurogenesis. J Comp
378 Neurol 425:479–494.

379 Rodin S, Domogatskaya A, Ström S, Hansson EM, Chien KR, Inzunza J, Hovatta O, Tryggvason K. 2010.
380 Long-term self-renewal of human pluripotent stem cells on human recombinant laminin-511.

381 Nat Biotechnol 28:611–615.

382 Schuler F, Sorokin LM. 1995. Expression of laminin isoforms in mouse myogenic cells in vitro and in
383 vivo. J Cell Sci 108:3795–805.

384 Shen Q, Wang Y, Kokovay E, Lin G, Chuang S-MM, Goderie SK, Roysam B, Temple S. 2008. Adult SVZ
385 stem cells lie in a vascular niche: a quantitative analysis of niche cell-cell interactions. Cell Stem
386 Cell 3:289–300.

387 Sixt M, Engelhardt B, Pausch F, Hallmann R, Wendler O, Sorokin LMM. 2001. Endothelial cell laminin
388 isoforms, laminins 8 and 10, play decisive roles in T cell recruitment across the blood–brain
389 barrier in experimental autoimmune encephalomyelitis. J Cell Biol 153:933.

390 Smyth N, Vatansever HS, Murray P, Meyer M, Frie C, Paulsson M, Edgar D. 1999. Absence of
391 Basement Membranes after Targeting the LAMC1 Gene Results in Embryonic Lethality Due to
392 Failure of Endoderm Differentiation. J Cell Biol 144:151–160.

393 Song J, Lokmic Z, Lämmermann T, Rolf J, Wu C, Zhang X, Hallmann R, Hannocks M-J, Horn N, Ruegg M
394 a, Sonnenberg A, Georges-Labouesse E, Winkler TH, Kearney JF, Cardell S, Sorokin L. 2013.
395 Extracellular matrix of secondary lymphoid organs impacts on B-cell fate and survival. Proc Natl
396 Acad Sci U S A 110:E2915–24.

397 Sorokin L. 1990. Recognition of the laminin E8 cell-binding site by an integrin possessing the alpha 6
398 subunit is essential for epithelial polarization in developing kidney tubules. J Cell Biol 111:1265–
399 1273.

400 Sorokin LM, Pausch F, Durbeej M, Ekblom P. 1997a. Differential expression of five laminin alpha (1-5)
401 chains in developing and adult mouse kidney. Dev Dyn 210:446–62.

402 Sorokin LM, Pausch F, Frieser M, Kröger S, Ohage E, Deutzmann R. 1997b. Developmental regulation
403 of the laminin alpha5 chain suggests a role in epithelial and endothelial cell maturation. Dev
404 Biol 189:285–300.

405 Tavazoie M, Van der Veken L, Silva-vargas V, Louissaint M, Colonna L, Zaidi B, Garcia-Verdugo JM,
406 Doetsch F, Veken L Van Der, Silva-vargas V, Louissaint M, Colonna L, Zaidi B, Doetsch F,
407 Procedures SE, {Van der Veken} L, Garcia-Verdugo JM, Van der Veken L, Silva-vargas V,
408 Louissaint M, Colonna L, Zaidi B, Garcia-Verdugo JM, Doetsch F. 2008. A Specialized Vascular
409 Niche for Adult Neural Stem Cells. Cell Stem Cell 3:279–288.

410 Thyboll J, Kortesmaa J, Cao R, Soininen R, Wang L, Iivanainen A, Sorokin L, Risling M, Cao Y,
411 Tryggvason K. 2002. Deletion of the Laminin 4 Chain Leads to Impaired Microvessel Maturation.
412 Mol Cell Biol 22:1194–1202.

413 Wegner J, Loser K, Apsite G, Nischt R, Eckes B, Krieg T, Werner S, Sorokin L. 2016. Laminin α5 in the
414 keratinocyte basement membrane is required for epidermal–dermal intercommunication.
415 Matrix Biol.

416 Wu C, Ivars F, Anderson P, Hallmann R, Vestweber D, Nilsson P, Robenek H, Tryggvason K, Song J,
417 Korpos E, Loser K, Beissert S, Georges-Labouesse E, Sorokin LM. 2009. Endothelial basement
418 membrane laminin alpha5 selectively inhibits T lymphocyte extravasation into the brain. Nat
419 Med 15:519–527.

420 Zhang Y, Huang G, Shornick LP, Roswit WT, Shipley JM, Brody SL, Holtzman MJ. 2007. A transgenic
421 FOXJ1-Cre system for gene inactivation in ciliated epithelial cells. Am J Respir Cell Mol Biol
422 36:515–9.

423

424 Figure Legends

425 **Figure 1**: Fractones are a major BM source in the SVZ and appear at the center of pinwheels. ***A***,
426 Whole mount of the lateral ventricle wall of an adult mouse immunofluorescently stained for laminin
427 γ1 (green). The frontal view reveals the profuse distribution of fractone bulbs at the neurogenic
428 niche. A higher magnification of the boxed area is depicted in the inset. ***B***, Frontal view of the

ependymal cell layer, seen at 1 µm depth relative to the ventricular surface, stained for laminin γ1 (green) to visualize fractones and β-catenin (red) to visualize ependymal cell junctions. All fractone bulbs sit at the interface between ependymal cells. ***C***, Maximum intensity projection of a Z-stack of a whole mount showing a GFAP+ NSC (gray) in contact with one blood vessel (yellow arrow) and more than 10 fractone bulbs (arrowheads) at the same time. ***D,*** The neural stem cell body also contacts a large bulb located at the center of a pinwheel (arrowhead). ***E***, Orthogonal views revealing that the NSC-fractone interaction seen in C-D occurs at the surface of a pinwheel center. ***F***, GFAP+ processes contact more bulbs at pinwheel centers (arrowheads) than bulbs at the basolateral surface of ependymal cells. Interactions between GFAP+ processes and fractone bulbs were labeled 1-3 and rendered, revealing that GFAP+ processes establish direct and complex contacts with fractones. Scale bars: A: 500 µm, inset: 200 µm. B-D: 25 µm. E: 12 µm. F: 25 µm.

Figure 2: Fractone bulbs are enriched in laminin α5. Immunolabeling for laminin α2 (red, top), laminin α4 (red, middle), laminin α5 (red, bottom) and laminin γ1 (green) showing that fractone bulbs and blood vessels have distinct laminin compositions and that laminin α5 is the main α chain in these structures, followed by a faint presence of laminin α2 (arrowheads). Asterisks indicate the ventricular cavity. Scale bars: 100 µm

Figure 3: Fractones emerge at the apical surface of ependymal cells in the first week after birth. ***A***, Coronal section of a newborn mouse showing scarce laminin expression (green) at the ependymal layer. ***B***, *In situ* hybridization of a sagittal section at the same age revealing extensive *Lama5* gene expression (gray in bottom panel, green in right panel) at the ependymal layer (arrow) and at the choroid plexus (arrowhead), weeks before protein is detected in blood vessels. ***C***, At day 3, laminin α5 is expressed in a more punctate pattern in several regions of the ependymal surface. ***D***, At day 7, early fractone bulbs can be clearly seen in all the ventricular surface. A frontal view of the ependymal

454 layer (***E***) shows fractones at the apical surface of ependymal cells, confirmed by orthogonal sections
455 of a confocal stack (***F***). ***G***, At the same time, laminin γ1 can be seen both as a punctate pattern at the
456 apical cell surface and a diffuse intracellular stain inside RFP+ ependymal cells in FoxJ1-RFP mice.
457 Asterisks indicate the ventricular cavity. Scale bars: A: 50 µm, B: 200 µm, higher magnification: 130
458 µm, C: 50 µm, D: 50 µm, E: 25 µm, F: 5 µm, G: 10 µm.

459

460 **Figure 4**: Fractones undergo major transformations with aging. ***A***, Fractones bulbs, identified by
461 immunofluorescent staining using a pan-laminin antibody (panLM) (top panel), at three different
462 ages. The volume of each individual bulb is color-coded, showing that these structures increase in
463 size with age. ***B***, The mean volumes of fractones correlate with age (R^2= 0.91, left panel). An analysis
464 of frequency showing that the median value for the volume of fractones also increases with age. ***C***, A
465 pinwheel in a whole mount of an 8 months old mouse showing a tunneled fractone bulb at its center.
466 Orthogonal views show a GFAP+ process (gray) sheathed by the fractone BM (green). ***D***, Unusually
467 large fractones (green, arrowheads) are associated with clusters of GFAP+ cells (gray, arrows). ***E***, A
468 detailed view of a cell cluster shows strong expression of β-catenin (red) in its margins and fractones
469 fragments (arrowheads) in its interior. ***F***, A tridimensional reconstruction of a giant fractone
470 associated with a cell cluster showing how GFAP+ processes transverse these structures. Scale bars:
471 A: 30 µm, C: 5 µm, D: 50 µm, E: 10 µm, F: 5 µm

472

473 **Figure 5**: Deletion of the *Lama5* gene in ependymal cells eliminates laminin α5 in fractones bulbs. ***A***,
474 Expression of laminin α5 (green) is not altered in mice lacking the *Lama5* gene in endothelial cells
475 (Tie2/*Lama5*$^{-/-}$), showing that these cells are not the source of the laminin α5 found in fractones. ***B***,
476 Analysis of the volume of fractones showing no difference in bulb size among these genotypes (data
477 are mean ± SEM, t-test n=3) ***C***, The vast majority of fractones in one month old FoxJ1/*Lama5*$^{-/-}$ lack
478 laminin α5, the main α chain in wild type animals. ***D***, One week old FoxJ1-RFP report mice, expressing

RFP upon FoxJ1 promoter activation, show that in some ependymal cells the FoxJ1 promoter is not active at one week after birth (arrowheads). ***E***, Lateral ventricle of a FoxJ1-RFP mouse showing the emergence of fractones at the apical surface of ependymal cells. At P7, the ventricle wall is lined by ependymal cells in different stages of maturation: ciliated RFP+ ependymal cells (*arrows*), non-ciliated RFP+ ependymal cells (*arrowheads*) and RFP- cells (*hollow arrowheads*) are present. ***F***, While most of the fractones are at the surface of RFP+ cells, some RFP– cells have fractones (arrowheads). Thin optical sections (0.3 µm) of RFP+ ependymal cells producing fractones at their apical membrane. ***G***, Two month old FoxJ1/*Lama5*$^{-/-}$ mice have no laminin α5 in fractone bulbs, instead, there is a compensatory upregulation of laminin α2 in these structures, (***H***) with a immunoreactivity similar to the blood capillaries in the vicinity (arrowheads). Scale bars: A: 25 µm, C: 25 µm, D: 100 µm, E: 25 µm, F: 10 µm, G: 20 µm, H: 20µm.

Figure 6 Laminin content of fractone bulbs affect cell proliferation in the SVZ. ***A***, Whole mounts of the lateral wall of the lateral ventricle of WT, FoxJ1/*Lama5*$^{-/-}$, Tie2/*Lama5*$^{-/-}$ and *Lama4*$^{-/-}$ mice were immunofluorescently stained for PH3, a mitosis marker. FoxJ1/*Lama5*$^{-/-}$ animals have a significant increase in the number of dividing cells comparing to wild type animals, quantified in ***B***. Dots represent individual wholemounts. Scale bars: A: 500 µm, high magnification: 50 µm.

Figure 7 Laminin in fractone bulbs affects proliferation in the SVZ. Neural stem cells (B cells, in blue) contact BMs from blood vessels (BV) and from fractones bulbs, which are produced by ependymal cells (E cells, in yellow). Fractone bulbs likely help the anchorage of NSC processes in the ependymal layer, including in the center of pinwheels. They are enriched in laminin α5 and changes in the laminin composition affect proliferation in the SVZ, most likely due changes in cell adhesion leading to activation of NSCs and generation of intermediary progenitors (C cells, in green) and neuroblasts

(A cells, in red). Laminin α5 is also found in the endothelial BM of blood vessels, but they are not accessible to neighboring cells since they are enclosed by the parenchymal BM.

Supplementary Figure 1 Interactions of GFAP+ processes with fractone bulbs at pinwheel centers. ***A***, Tridimensional reconstruction of the pinwheel seen in Fig.1*C-E*, showing the interactions of a NSC body with a bulb at the pinwheel center and its processes reaching several other fractones. ***B***, Orthogonal views of the image seen in Fig. 1F, confirming that fractone bulbs sit between ependymal cells at pinwheel centers and GFAP+ processes directly contact them. Scale bars: A: 50 µm, B: 12 µm.

Supplementary Figure 2 The emergence of fractones bulbs is spatially heterogeneous. At P3, the first fractones appear at the ventricle wall (*arrow*), seen as a punctate expression of laminin γ1, while most of the walls are devoid of laminins (*arrowhead*). Boxes are higher magnifications of the indicated areas. Scale bar: 50 µm, higher magnification: 20 µm

Supplementary Figure 3 Laminin content of endothelial BM do not affect cell proliferation in the SVZ. Whole mounts of the lateral wall of Tie2Cre/*Lama5*$^{-/-}$, a lineage that does not express laminin α5 in endothelial cells and Lama4$^{-/-}$, a lineage with a compensatory overexpression of laminin α5 in the endothelium, were prepared and immunofluorescently labeled for PH3. These lineages showed a proliferative pattern at the SVZ similar to wild type animals. Scale bars: A: 500 µm, high magnification: 50 µm**.**

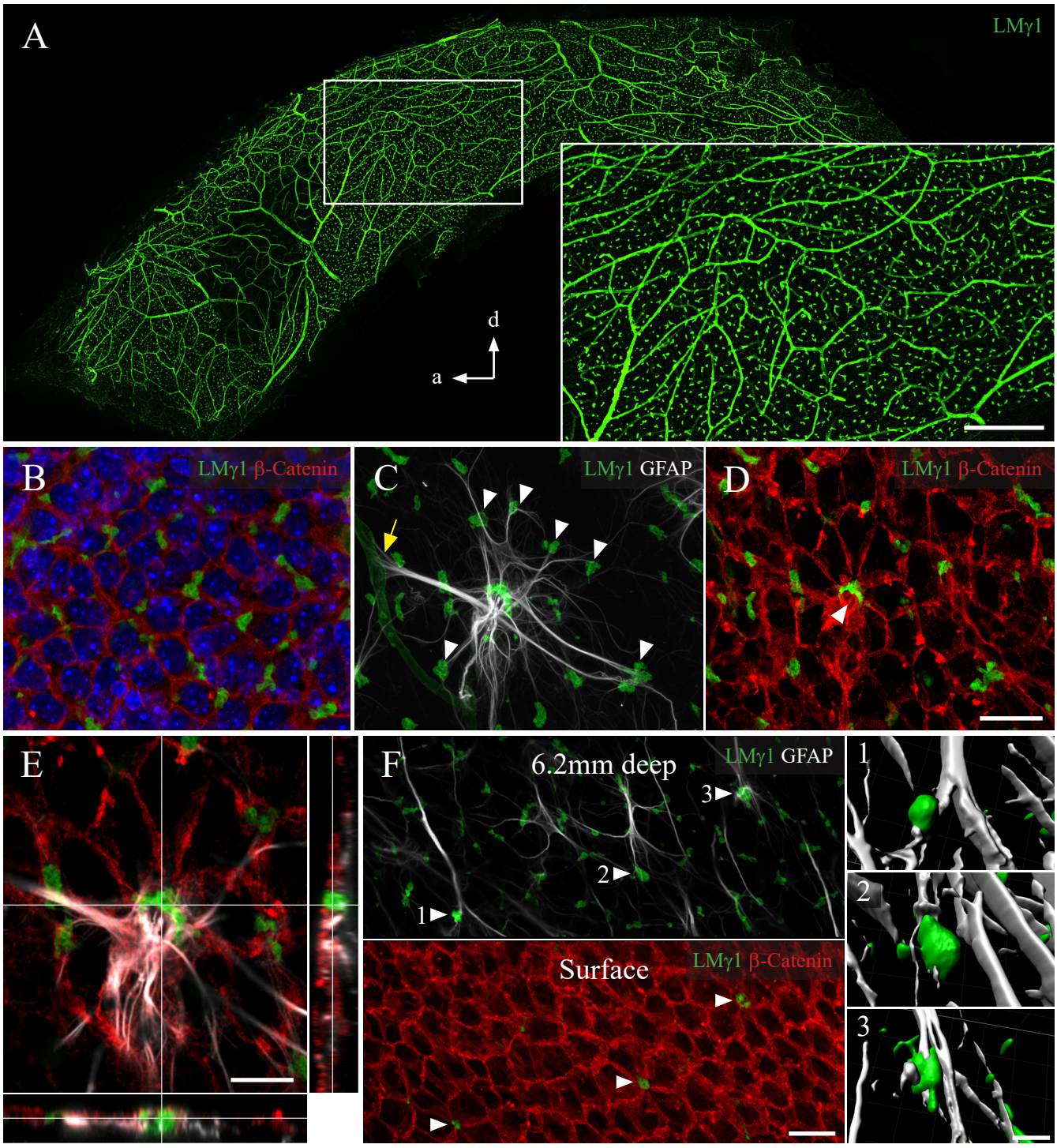
A
LMγ1
d
a
B
LMγ1 β-Catenin
C
LMγ1 GFAP
D
LMγ1 β-Catenin
E
F
6.2mm deep
LMγ1 GFAP
1
2
3
Surface
LMγ1 β-Catenin
1
2
3

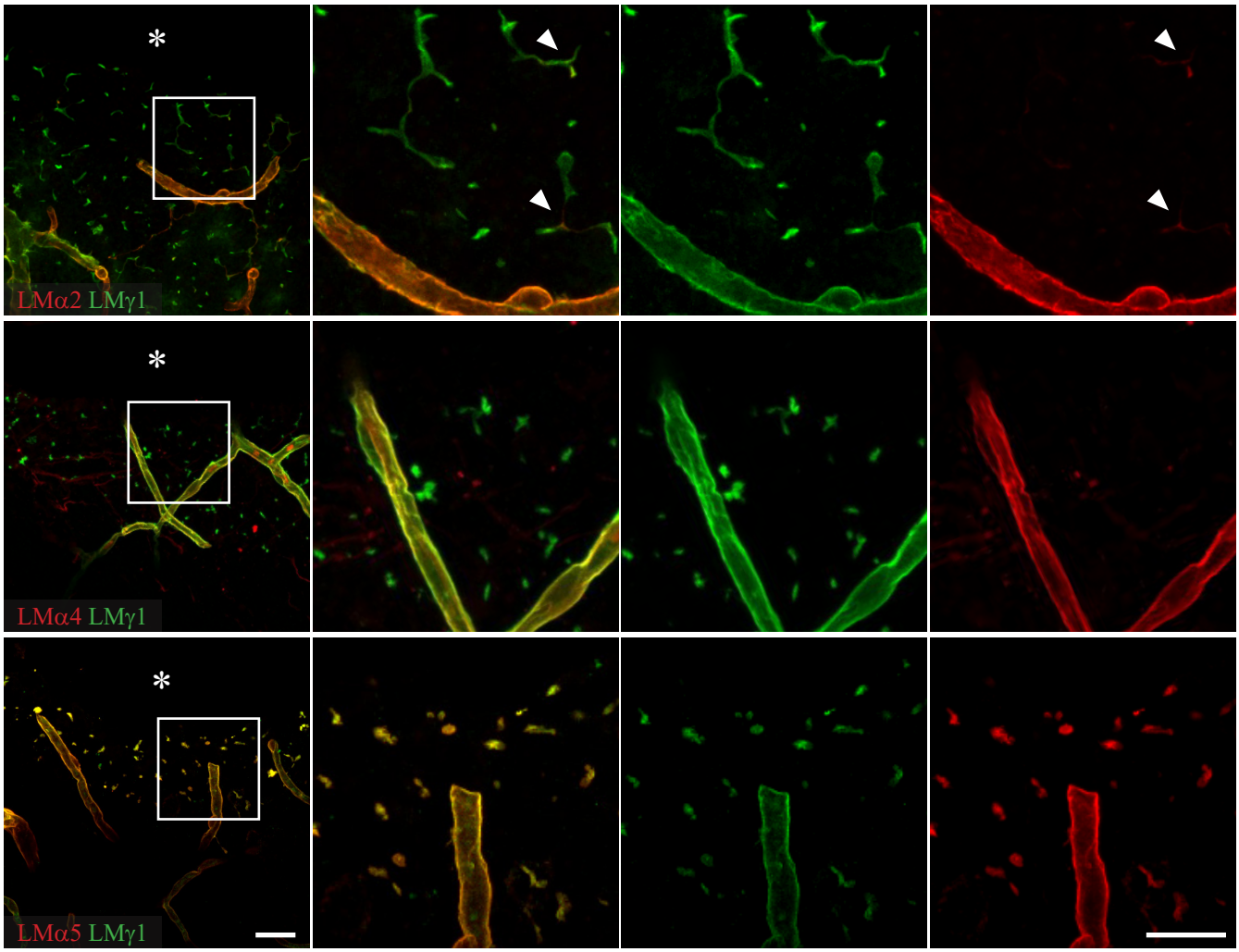
LMα2 LMγ1
LMα4 LMγ1
LMα5 LMγ1

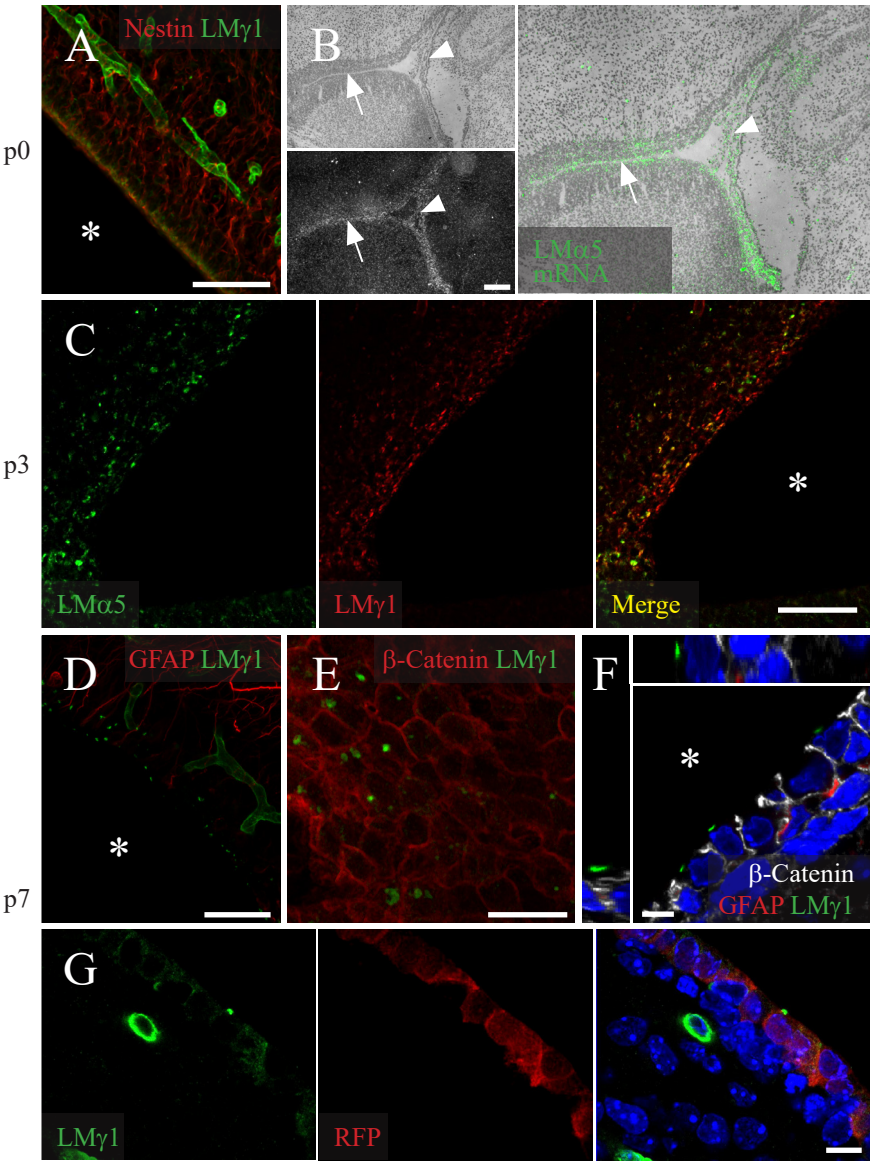
p0
A
Nestin LMγ1
*
B
LMα5
mRNA
p3
C
LMα5
LMγ1
Merge
*
p7
D
GFAP LMγ1
*
E
β-Catenin LMγ1
F
*
β-Catenin
GFAP LMγ1
G
LMγ1
RFP

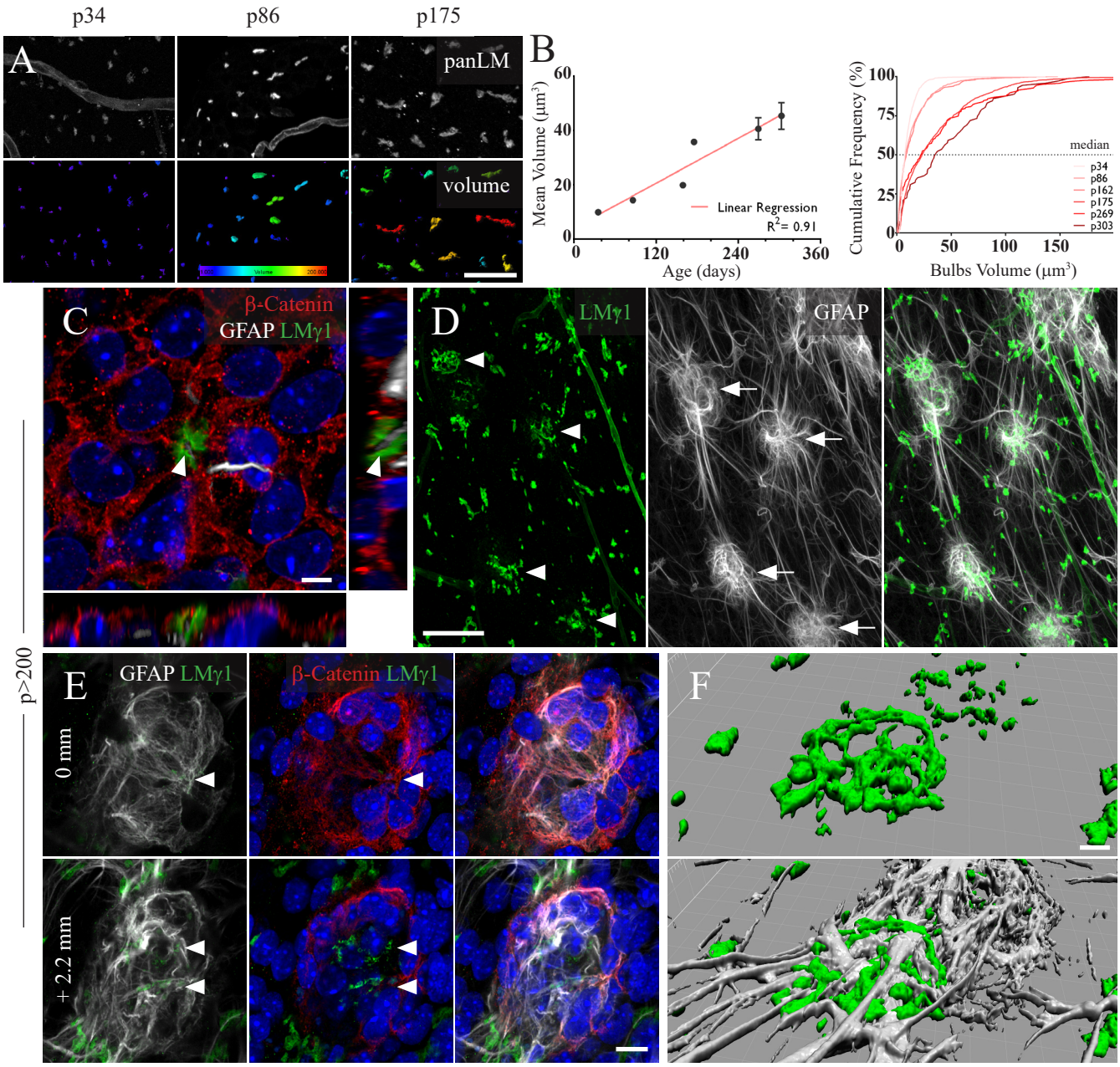
p34
p86
p175
A
panLM
volume
B
Mean Volume (µm³)
Age (days)
Linear Regression
R²= 0.91
Cumulative Frequency (%)
median
p34
p86
p162
p175
p269
p303
Bulbs Volume (µm³)
C
β-Catenin
GFAP LMγ1
D
LMγ1
GFAP
p>200
E
GFAP LMγ1
β-Catenin LMγ1
0 mm
+ 2.2 mm
F

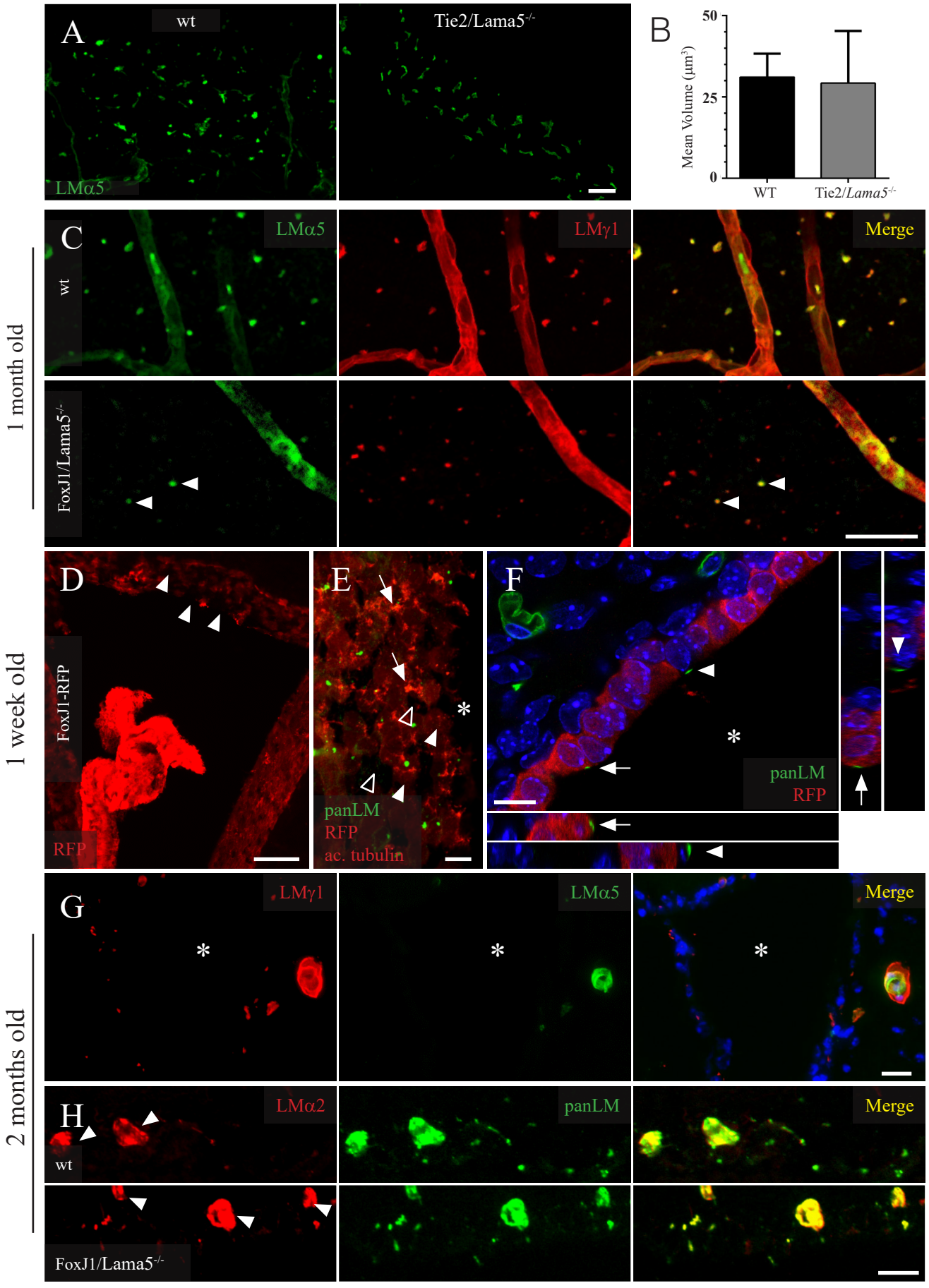
A
wt
Tie2/Lama5-/-
LMα5
B
Mean Volume (μm3)
50
25
0
WT
Tie2/Lama5-/-
C
wt
LMα5
LMγ1
Merge
FoxJ1/Lama5-/-
1 month old
D
FoxJ1-RFP
RFP
E
panLM
RFP
ac. tubulin
F
panLM
RFP
1 week old
G
LMγ1
LMα5
Merge
H
wt
LMα2
panLM
Merge
FoxJ1/Lama5-/-
2 months old

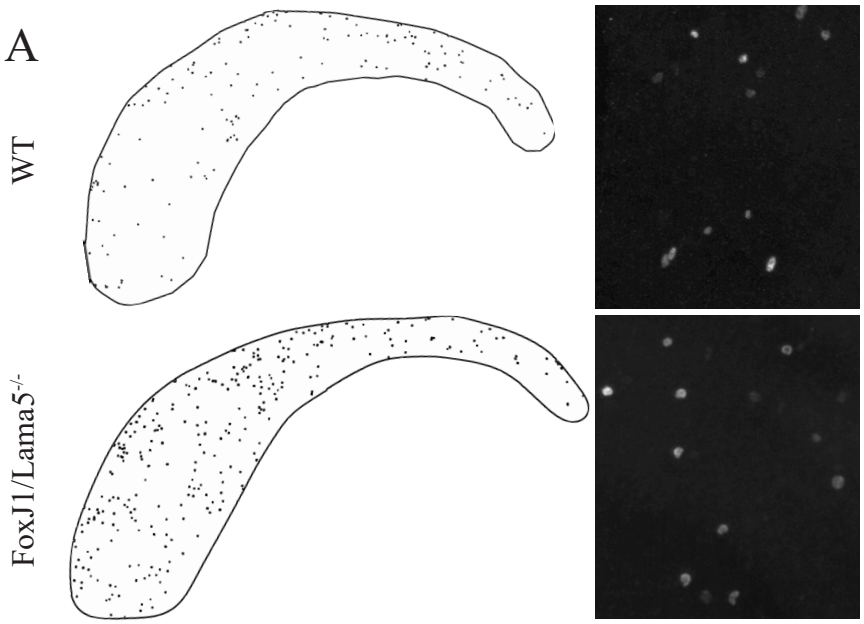
A
WT
FoxJ1/Lama5-/-

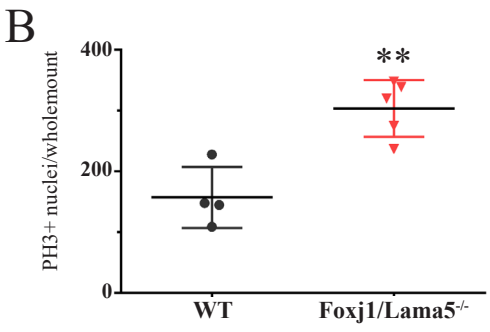
B
PH3+ nuclei/wholemount
400
200
0
**
WT
Foxj1/Lama5-/-

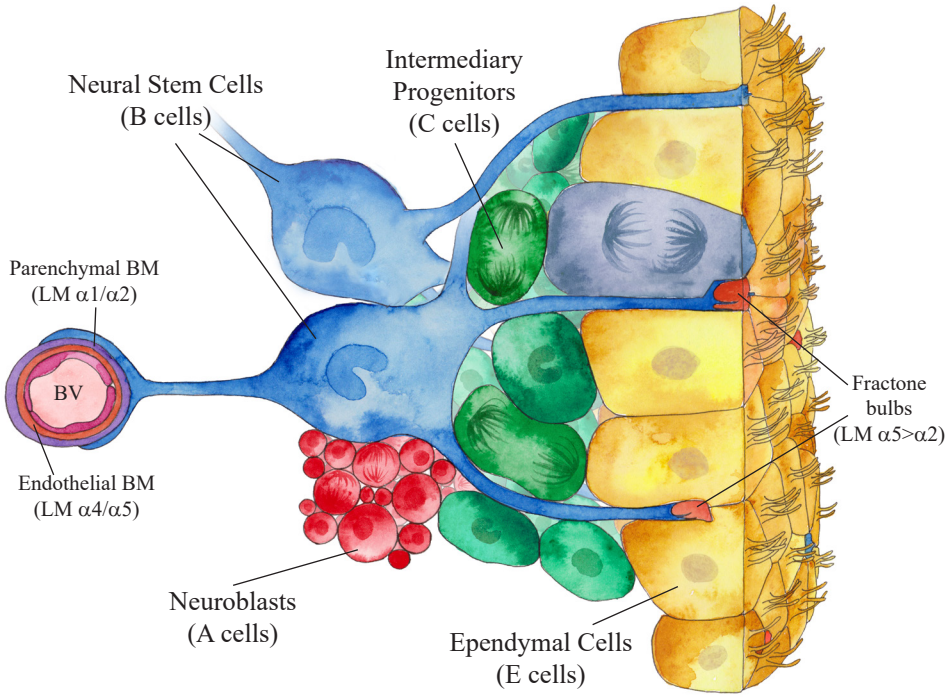
Neural Stem Cells
(B cells)
Intermediary
Progenitors
(C cells)
Parenchymal BM
(LM α1/α2)
BV
Endothelial BM
(LM α4/α5)
Fractone
bulbs
(LM α5>α2)
Neuroblasts
(A cells)
Ependymal Cells
(E cells)